The Observation and Interpretation of some Properties of $SmCo_5$ Permanent Magnet Alloys

by

C.K.Mylvaganam

A thesis submitted to the Faculty of Graduate Studies of the University of Manitoba in partial fulfilment of the requirements for the degree of Doctor of Philosophy.

Department of Physics
University of Manitoba
June, 1980

THE OBSERVATION AND INTERPRETATION OF SOME PROPERTIES OF $SmCo_5$ PERMANENT MAGNET ALLOYS

BY

CHANDRARAJ KANTHA MYLVAGANAM

A thesis submitted to the Faculty of Graduate Studies of the University of Manitoba in partial fulfillment of the requirements of the degree of

DOCTOR OF PHILOSOPHY

©/1980

Permission has been granted to the LIBRARY OF THE UNIVERSITY OF MANITOBA to lend or sell copies of this thesis, to the NATIONAL LIBRARY OF CANADA to microfilm this thesis and to lend or sell copies of the film, and UNIVERSITY MICROFILMS to publish an abstract of this thesis.

The author reserves other publication rights, and neither the thesis nor extensive extracts from it may be printed or otherwise reproduced without the author's written permission.

Acknowledgements

I am indebted to my supervisor, Professor Paul Gaunt, who actively participated in this research project, making a substantial contribution to its successful completion.

I am grateful to Mr. Gilles Roy, who willingly made available his vast store of expertise on experimental matters whenever it was requested.

Thanks are also due to Ms. Yuen Cheng, who assisted me with some aspects of the computer programming and to Mr. Greg Kenning, who analysed some of the X-ray data.

Finally, I would like to express my deep appreciation of the understanding and encouragement afforded me throughout the duration of this project by my wife, Ruvani, who also did such an excellent job of typing this thesis.

Abstract

The high coercive force of liquid-phase sintered $SmCo_5$ alloys is associated with grain boundary inhomogeneities. In the demagnetized initial state, on cooling from the Curie temperature, a uniaxial material such as $SmCo_5$ will contain several 180^o domain walls. Upon application of a forward field, neighbouring 180^o walls will approach each other and, depending on their relative sense of spin rotation, will either be annihilated or form a tightly wound 360^o wall. In the presence of an inhomogeneous region with a lower wall energy than the matrix, the 360^o wall may be pinned, forming a nucleation centre which requires a large reverse field to unpin it and regenerate the two original 180^o walls.

The interaction between a 360^o wall and a localized planar inhomogeneity is treated micromagnetically to develop a model which minimizes the activation energy.

Measurements of magnetization and Barkhausen effect confirm that in sintered $SmCo_5$, domain walls are pinned at highly localized sites which coincide with grain boundaries. The model is therefore applied to this material, assuming a planar Sm_2Co_{17} inhomogeneity. Calculations are performed for inhomogeneity thicknesses up to 125Å at temperatures varying from 4.2K to 500K. Coercive fields that agree closely with experimental determinations are obtained. A critical inhomogeneity thickness (17Å at 77K) below which the coercivity disappears is determined at each temperature. Above this thickness, coercivity rises

steeply until it reaches a plateau. It is observed that more than one pair of walls can exist within the grain.

The interaction between an inhomogeneity and a domain wall may be described by a parabolic force, which gives a two-thirds power relationship between activation energy and field. A similar power relationship is exhibited by the activation energy calculated from the micromagnetic model.

The possibility that the continuously pinned wall's escape may be facilitated by thermal activation is considered. It is suggested that the wall bows out, forming a thermally activated 'blister', before breaking away at a smaller field than might otherwise be expected. The activation energy/field parameter, $(\frac{\partial E}{\partial H})_T$, is determined by combining the micromagnetic and parabolic force theories.

Measurements of magnetic after-effect made at temperatures from 4.2K to room temperature, over a range of effective fields to 20kOe, reveal the presence of a range of activation energies within the material. $(\frac{\partial E}{\partial H})_T$ is obtained at each field and is seen to extrapolate towards the theoretical value at the predicted coercive field. It is further observed that even though the viscosity coefficient is dependent on specimen history, $(\frac{\partial E}{\partial H})_T$ depends only on the effective field present.

The presence of non-stoichiometric phases which have different crystalline anisotropies is consistent with the observed relationship between H_{eff} and $(\frac{\partial E}{\partial H})_T$.

TABLE OF CONTENTS

CHAPTER 1

INTRODUCTION

1.1 Domains and Domain Walls

Ferromagnets are defined as those materials in which atomic dipole moments are aligned parallel to one another. Such materials can therefore exhibit a magnetic moment even in the absence of a field. Despite this property of spontaneous magnetization, a ferromagnet which has not been exposed to a magnetic field will not exhibit a magnetic moment. Upon the application of even a small field however, a large moment may be seen.

To explain these phenomena, Weiss (1907) postulated the existence of small spontaneously magnetized regions, which he called 'domains', within the material. These domains would have individual magnetic moments, but could be aligned in such a manner as to give a null resultant moment over the whole material. When a field was applied, they would realign themselves, giving a new resultant moment. Such a multi-domain configuration has, in general, a lower magnetostatic energy than a single region of uniform magnetization over the entire material. (When the material is sufficiently small however, the single domain configuration is the preferred one.)

The region between adjacent domains is one in which atomic moments are in the process of changing direction, as shown in figure 1.1-1. This boundary layer is known as a 'domain wall'. Realignment of domains is therefore characterized by movement of domain walls.

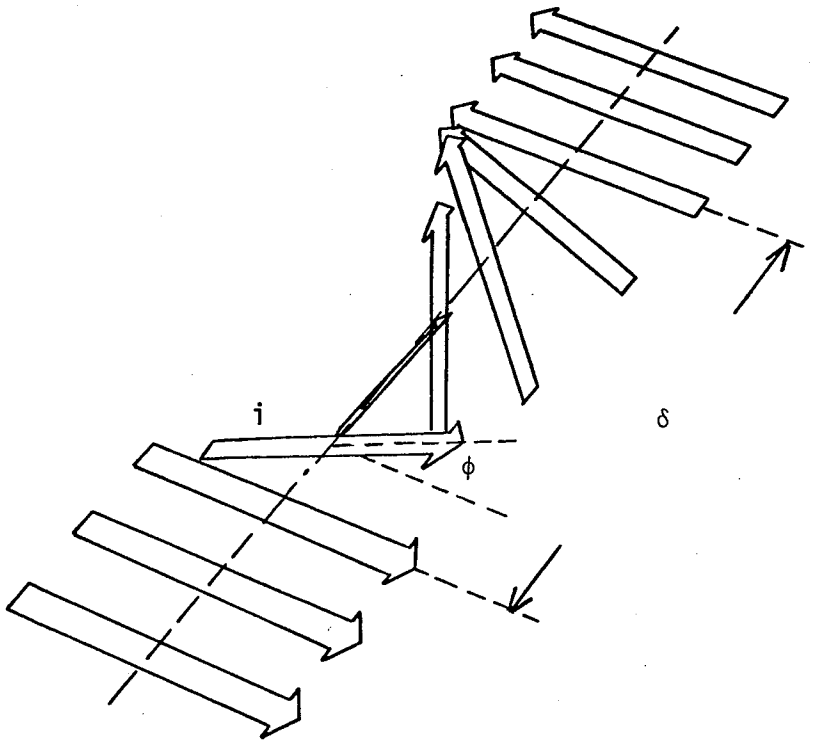

Figure 1.1-1 - A 180° domain wall of width δ. The spins are rotating out of the plane of magnetization. The i^{th} spin has rotated by an angle ϕ.

1.2 Magnetic Hardening

1.2.1 Introduction

When a material has been magnetized to saturation, it can be demagnetized by applying a field in the direction opposite to that of the moment. The required field is known as the 'coercive field'. A large coercive field is a characteristic of 'hard' magnetic materials. While the boundary between hard and soft materials is not precisely defined, a coercive field of 50 Oe is generally regarded as being indicative of magnetic hardness. Plainly, the harder the material, the more desirable it is as a permanent magnet.

If a material is magnetically hard, it is difficult to change its domain configuration or to move its domain walls from their static positions. Magnetic hardening must therefore be characterized by a mechanism which keeps the wall 'pinned' or 'trapped' until the coercive field is applied. Many theories of magnetic hardening have been suggested and the following is a brief description of some of them.

1.2.2 Reversal of Single Domain Particles

Stoner and Wohlfarth (1948) have studied the difficulty of reversing single domain particles if they have initially been magnetized in the easy direction of the material. Here the change in anisotropy energy has to be overcome by the energy contributed by the magnetic field and when this energy is attained at the coercive field the magnetization will flip around.

1.2.3 Non-Ferromagnetic Inclusions

The effect on coercivity of non-ferromagnetic inclusions within a ferromagnetic matrix was examined by Kersten (1943) in his study of copper and carbon inhomogeneities in iron. He looked at the effect on the energy of the domain wall when it intersected an inclusion. Since the inclusion was non-magnetic, this in effect shortened the wall, decreasing its energy and therefore placed it in an energy state which was preferable to the one where it did not intersect an inclusion. The wall would thus remain pinned by the inclusion until a sufficiently large field was applied.

Consider a matrix of saturation magnetization I per unit volume and containing n inclusions per unit volume which are spherical, with radius r, occupying the corners of a cubic lattice. A wall of unit area will therefore intersect $n^{2/3}$ inclusions.

Initially the wall is in a pinned state, lying across the middle of the plane of inclusions as shown in figure 1.2.3-1a. When a field H is applied, the wall is displaced a distance x as in figure 1.2.3-1b.

The change in wall area per inclusion is

$$\pi r^2 - \pi(r^2 - x^2).$$

If γ is the wall energy per unit area, the change in wall energy per unit area is $n^{2/3}\gamma\pi x^2$.

When the wall is displaced by x, this means that a volume of x per unit area has reversed magnetization. The corresponding change in

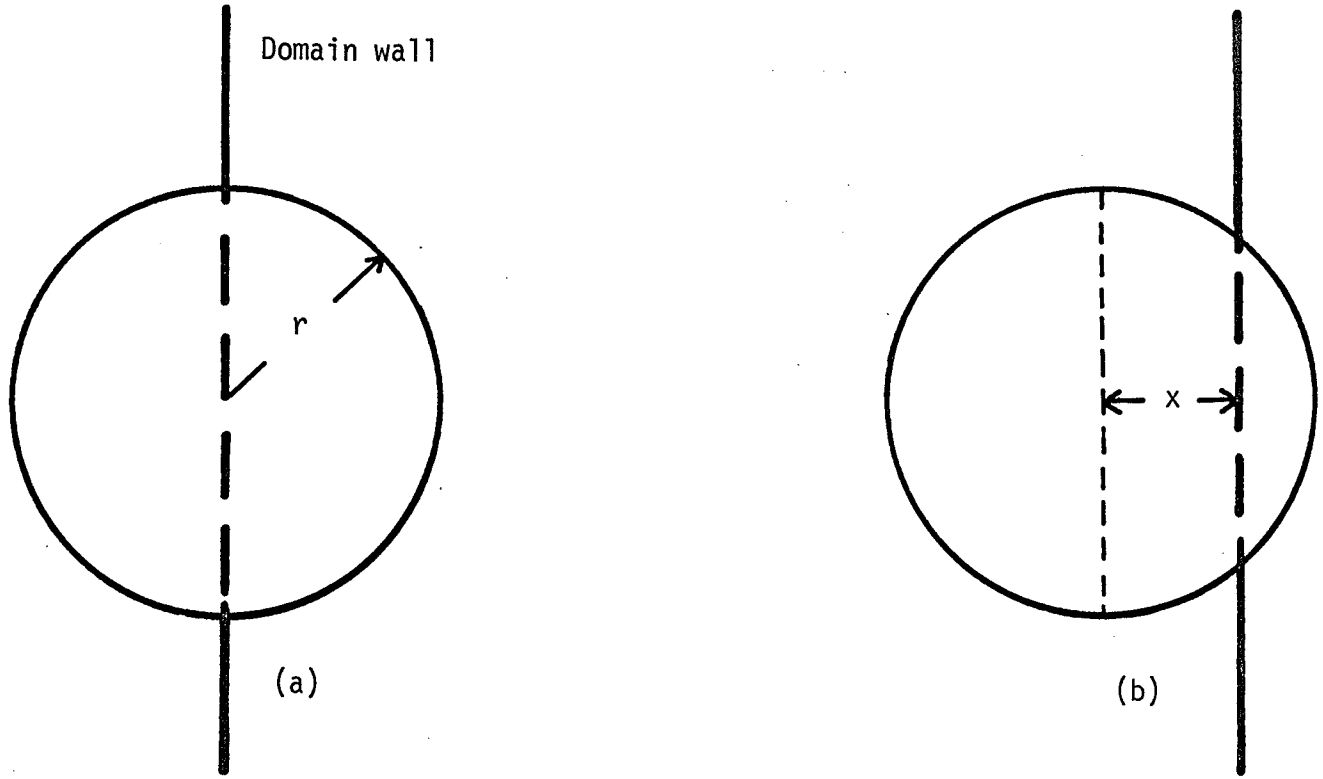

Figure 1.2.3-1 - (a) Domain wall pinned by an inclusion in the absence of a field.
(b) Wall has been displaced by the application of a field.

energy per unit area is $2HIx$.

The total energy per unit area,

$$\Delta E = n^{2/3}\pi\gamma x^2 - 2HIx \ .$$

Since this must be minimized,

$$\frac{\partial(\Delta E)}{\partial x} = 0$$

and this gives,

$$H = \frac{\pi n^{2/3} \gamma}{I} x \ .$$

Displacement is therefore proportional to the field as long as the wall is being intersected. The field required so that wall may reach the edge of the inclusions is

$$H_c = \frac{\pi n^{2/3} \gamma}{I} x \ ,$$

and this must be the coercive field because once the wall has passed through the inclusions, it is free to continue moving through the material until it reaches the next plane of obstacles. Since all inclusions are the same size, this field should be sufficient to enable the wall to move freely through the entire material.

This theory yielded satisfactory correlation with experimental observations in cases where the dimensions of the obstacle were much greater than the width of the domain wall.

1.2.4 Ferromagnetic Inclusions

Kersten's theory can, with the appropriate modifications, be extended to the case of ferromagnetic inclusions within a ferromagnetic

matrix. Pinning can take place in such a situation if the domain wall energy within the inclusion is lower than that within the matrix. The wall will then have a lower energy if it intersects inclusions and will prefer to remain in this state.

Conversely, an inclusion with a higher energy will act as an obstacle, blocking the path of the wall.

1.2.5 Free Poles

Néel (1946) criticized Kersten's theory on the grounds that even though inclusions would be expected to have free poles on their surfaces, producing disperse fields with large magnetostatic energies, their presence had been ignored. The presence of random strains in the material could cause changes in the easy direction of magnetization, producing further free poles and these should have been considered as well.

Neel showed that the logarithm of the coercive field varied linearly with the logarithm of the volume fraction of inclusions and compared his theoretical values with experimental results for many systems.

1.3 The Present Study

In the present study, the processes governing magnetic hardening in sintered $SmCo_5$ permanent magnet alloys were examined. Craik and Hill (1974) have suggested that magnetic hardening in rare earth-cobalt materials may be caused by the insertion within the material of planes

having different exchange and anisotropy energies. As detailed more fully by other authors (chapter 2), $SmCo_5$ alloys may be expected to contain other phases of Sm-Co compounds, such as Sm_2Co_{17} and Sm_2Co_7, which are also ferromagnetic. An order of magnitude calculation indicated negligible demagnetizing effects due to inhomogeneities within the matrix. A theory of coercivity in which domain walls were pinned by planar inclusions of a secondary phase was therefore developed. The remainder of this section seeks to outline the path taken to develop and to substantiate this model.

A model describing the interaction between a 180° domain wall and a planar inhomogeneity was synthesized (chapter 3). This gave expressions for the distribution of energy barriers and the effect of thermal activation.

In chapter 4 expressions for the energy of a domain wall in an $SmCo_5$ matrix as it interacted with planar Sm_2Co_{17} inhomogeneities were derived using a micromagnetic approach and values for the coercive field were obtained. These were compared with the experimental determinations of coercivity in chapter 6 as well as those contained in other studies.

The validity of the interaction model was tested by comparing the energy barrier distribution obtained from the purely theoretical calculation of chapter 3 with the values from the magnetic after-effect experiments of chapter 7. This, being a direct evaluation, gives a much better indication of barrier distribution than the measurements of coercive field, because the effect of thermal activation on coercivity itself is relatively small.

The model was based on the premise that pinning took place only at inhomogeneities and that there was free movement of domain walls within the grain. This was verified with further magnetization measurements to study the reversibility of domains (chapter 6), as well as by measurements of Barkhausen jumps (chapter 8) which were correlated with the grain size measurements of chapter 5.

X-ray diffraction and electron microscopy were used to positively identify the material used, as well as to yield information on the nature and distribution of any inhomogeneities that may have been present (chapter 5).

The above is a brief outline of the procedure that was followed in this investigation. It is, along with the findings, detailed fully in the following chapters. The results are discussed in chapter 9.

CHAPTER 2

SAMARIUM-COBALT MAGNET MATERIAL

2.1 Introduction

$SmCo_5$ has found widespread use as a commercial magnet because of its desirable permanent magnet characteristics which include large coercivities and $(BH)_{max}$ energy products. Interestingly, these properties are not exhibited by the bulk alloy, but by small particles of the material. They are further enhanced when the particles are aligned and compacted to a high density.

The $SmCo_5$ magnets used in this study were manufactured in this manner. This chapter therefore examines the structure of the material, the process of manufacture, the likelihood of the presence of secondary phases and the structure of such phases.

2.2 Structure of $SmCo_5$

Crystals of $SmCo_5$ have alternate layers as shown in figure 2.2-1. One type of layer has a hexagonal arrangement of Co atoms. The other has Sm and Co atoms in a 1:2 ratio. The structure, which is hexagonal, belongs to the P6/mmm space group with the following atomic co-ordinates for the unit cell:

$$\text{Sm} - (0\ 0\ 0)$$

$$\text{Co} - (\tfrac{1}{3}\ \tfrac{2}{3}\ 0), (\tfrac{2}{3}\ \tfrac{1}{3}\ 0)$$

$$(\tfrac{1}{2}\ 0\ \tfrac{1}{2}), (0\ \tfrac{1}{2}\ \tfrac{1}{2}), (\tfrac{1}{2}\ \tfrac{1}{2}\ \tfrac{1}{2})$$

as given by the International tables for X-ray crystallography, Volume I (1969).

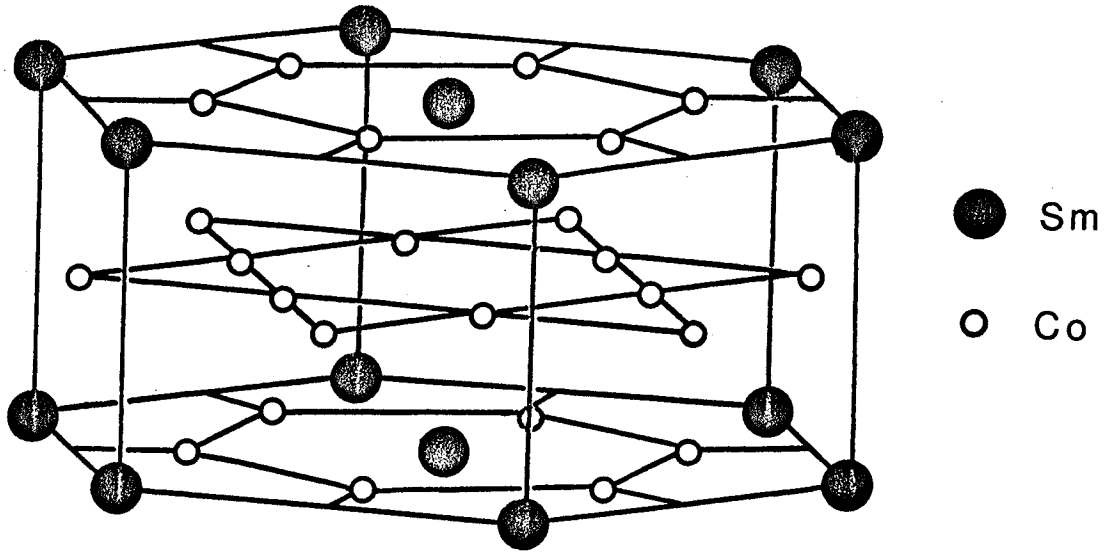

Figure 2.2-1 - Structure of $SmCo_5$.

Typical lattice parameters, according to Taylor (1971), are $a = 4.989\text{Å}$, $c = 3.981\text{Å}$.

2.3 Manufacture of the Magnets

Two techniques have been used for the densification of $SmCo_5$ powders. The first is the process of mechanical compaction, which was successfully carried out by Buschow, Luiten and Westendorp (1969). They aligned loosely packed $SmCo_5$ powder in a magnetic field and pressed it to a relative density of 70%. It must be noted that it is essential to have initial loose packing so that the particles may rotate easily. Further compression under a hydrostatic pressure of 20 kbars, combined with uniaxial deformation, increased relative density to over 95%. This process gives the desired permanent magnet properties, but because of the high pressures that are required, the size of the magnet is restricted.

The other is the technique of bonding the aligned particles by heating them, known as sintering. A problem here was that stoichiometric $SmCo_5$ underwent a loss of coercivity during the sintering process, as reported by Cech (1970). Benz and Martin (1970) overcame this by combining two melts at 1100°C. The first was stoichiometric with 66.7 wt.% Co, while the second, which was in its liquid phase at this temperature, has 40 wt.% Co. They were mixed to an average composition of 62.6 wt.% Co, which corresponds to 81 at.% Co. After aligning and pressing to 13 kbars, the powder was sintered at 1100°C for 30 minutes. Relative densities of 90 to 95% were obtained in this manner. Such a process is known as liquid phase sintering.

Das (1969) used a single melt with 63 wt.% Co instead of a combination of melts as described above.

The sintering temperature and time are critical in determining the permanent magnet properties of the alloy. Further heat treatment of the sintered magnet is carried out to enhance them.

2.4 Secondary Phases

2.4.1 Formation

The cobalt-rich portion of the Sm-Co phase diagram (Buschow and den Broeder 1973) is reproduced in figure 2.4.1-1. It is evident that small variations in the stoichiometry of the alloy will give rise to secondary cobalt-rich Sm_2Co_{17} or samarium-rich Sm_2Co_7 phases. Indeed, the presence of secondary phases is almost unavoidable, because if a single stoichiometric powder is used, heavy oxidation of the samarium will lead to the formation of a cobalt-rich phase (Jorgensen and Bartlett 1973), whereas the mixing of hypostoichiometric and stoichiometric powders in the liquid phase sintering process will give an initially samarium-rich phase which, depending on the degree of oxidation of samarium can even become cobalt-rich. The post-sintering annealing to which the material is subjected can cause some further decomposition of the primary $SmCo_5$ phase. This eutectoid decomposition has been studied by den Broeder and Buschow (1972) and Martin and Smeggil (1973). The effect of these secondary phases on magnetic properties has been examined by den Broeder and Zijlstra (1976) and will be discussed in the final chapter.

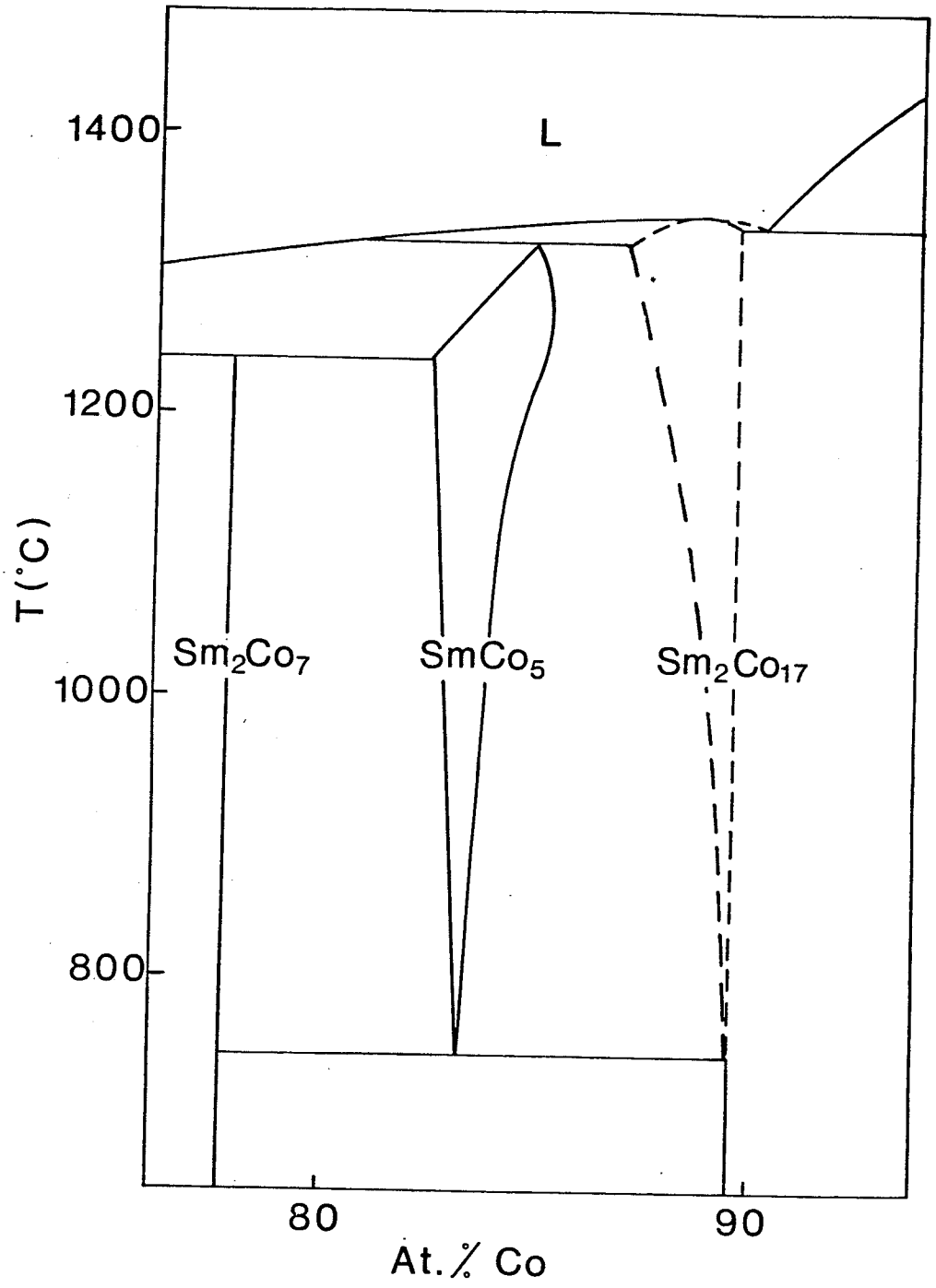

Figure 2.4.1-1 - Co-rich portion of the Sm-Co phase diagram (Buschow and den Broeder 1973).

2.4.2 Structure of Sm_2Co_{17}

Sm_2Co_{17} can have either a hexagonal or a rhombohedral structure. The hexagonal lattice is formed from the $SmCo_5$ lattice by having an ordered sublattice of a pair of Co atoms for every third Sm atom, followed by a [0 1 0] alternate sense stacking shift on every second (0 0 1) layer. This is illustrated in figure 2.4.2-1 (Ostertag, Strnat and Hoffer 1967). The rhombohedral structure, which is formed if the stacking displacement is not reversed, is illustrated in figure 2.4.2-2 (Ostertag et al 1967). The basal 'a' axes of the Sm_2Co_{17} unit cell are rotated by 30° with respect to those of the original $SmCo_5$ cell. 'a' is increased by a factor of $\sqrt{3}$. 'c' is doubled. Taylor (1971) gives lattice parameters for Sm_2Co_{17} as a = 8.402Å and c = 8.114Å (hexagonal) or 12.172Å (rhombohedral).

In the ITXC (v.I) notation, Ostertag et al (1967) have shown that the hexagonal Sm_2Co_{17} unit cell belongs to the $P6_3/mmc$ space group and has the following positions occupied:

Sm(1) - $\pm(0\ 0\ \frac{1}{4})$

Sm(2) - $\pm(\frac{1}{3}\ \frac{2}{3}\ \frac{3}{4})$

Co(1) - $\pm(\frac{1}{3}\ \frac{2}{3}\ z)$, $\pm(\frac{2}{3}\ \frac{1}{3}\ \frac{1}{2}+z)$

Co(2) - $(\frac{1}{2}\ 0\ 0)$, $(0\ \frac{1}{2}\ 0)$, $(\frac{1}{2}\ \frac{1}{2}\ \frac{1}{2})$,$(\frac{1}{2}\ \frac{1}{2}\ 0)$,$(\frac{1}{2}\ 0\ \frac{1}{2})$,$(0\ \frac{1}{2}\ \frac{1}{2})$

Co(3) - $\pm(x\ y\ \frac{1}{4})$, $\pm(\bar{y}\ x\text{-}y\ \frac{1}{4})$, $\pm(y\text{-}x\ \bar{x}\ \frac{1}{4})$, $\pm(\bar{y}\ \bar{x}\ \frac{1}{4})$, $\pm(x\ x\text{-}y\ \frac{1}{4})$, $\pm(y\text{-}x\ y\ \frac{1}{4})$

Co(4) - $\pm(x\ 2x\ z)$, $\pm(2\bar{x}\ \bar{x}\ z)$, $\pm(x\ \bar{x}\ z)$, $\pm(\bar{x}\ 2\bar{x}\ \frac{1}{2}+z)$, $\pm(2x\ x\ \frac{1}{2}+z)$, $\pm(\bar{x}\ x\ \frac{1}{2}+z)$